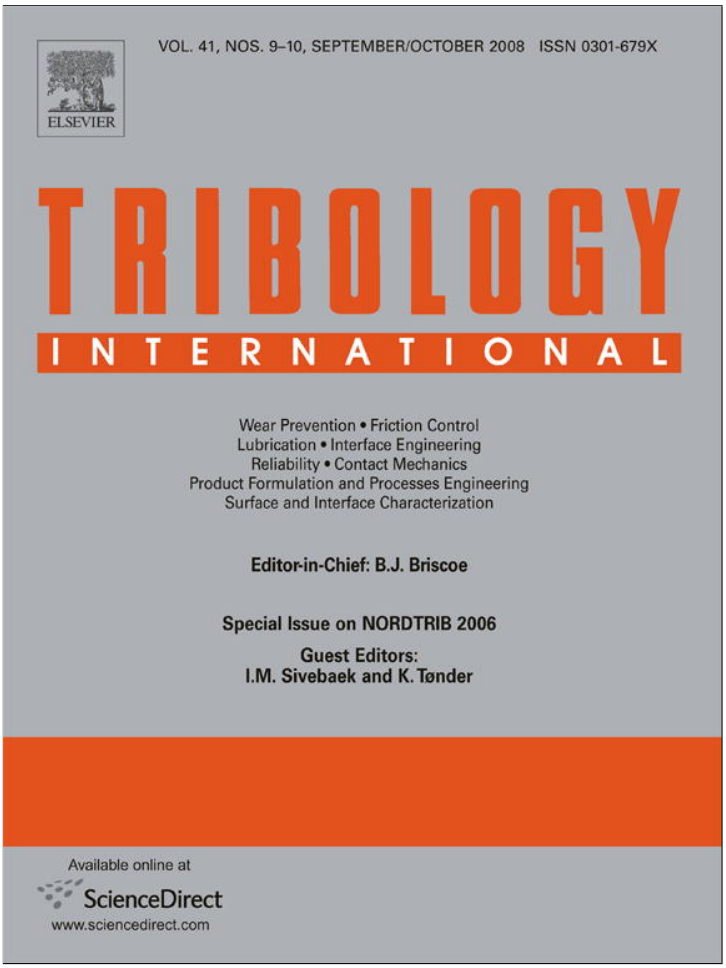

Available online at www.sciencedirect.com
ScienceDirect
Tribology International 41 (2008) 920–925
TRIBOLOGY INTERNATIONAL
www.elsevier.com/locate/triboint

Lubricated friction between incommensurate substrates

A. Vanossi[a,*], G.E. Santoro[b,c], N. Manini[d], E. Tosatti[b,c], O.M. Braun[e]

[a]CNR-INFM National Research Center S3 and Department of Physics, University of Modena and Reggio Emilia, Via Campi 213/A, 41100 Modena, Italy
[b]International School for Advanced Studies (SISSA) and INFM Democritos National Simulation Center, Via Beirut 2, I-34014 Trieste, Italy
[c]International Centre for Theoretical Physics (ICTP), P.O. Box 586, I-34014 Trieste, Italy
[d]Department of Physics, University of Milan, Via Celoria 16, 20133 Milan, Italy
[e]Institute of Physics, National Academy of Sciences of Ukraine, 03028 Kiev, Ukraine

Received 30 January 2007; received in revised form 14 November 2007; accepted 15 November 2007
Available online 26 December 2007

Abstract

This paper is part of a study of the frictional dynamics of a confined solid lubricant film—modelled as a 1D chain of interacting particles confined between two ideally incommensurate substrates, one of which is driven relative to the other through an attached spring moving at constant velocity. This model system is characterized by *three* inherent length scales; depending on the precise choice of incommensurability among them it displays a strikingly different tribological behavior. Contrary to *two* length-scale systems such as the standard Frenkel–Kontorova (FK) model, for large chain stiffness one finds that here the most favorable (lowest friction) sliding regime is achieved by chain-substrate incommensurabilities belonging to the class of non-quadratic irrational numbers (e.g., the spiral mean). The well-known golden-mean (quadratic) incommensurability which slides best in the standard FK model shows instead higher kinetic friction values. The underlying reason lies in the pinning properties of the lattice of solitons formed by the chain with the substrate having the closest periodicity, with the other slider.

Keywords: Nanotribology; Friction; Models of nonlinear phenomena; Lubrication

1. Introduction

Nonlinear systems driven far from equilibrium exhibit a very rich variety of complex spatial and temporal behavior. In particular, in the emerging field of nanoscale science and technology, understanding the nonequilibrium dynamics of systems with many degrees of freedom which are pinned in some external potential, as commonly occurs in solid-state physics, is becoming more and more a central issue. Classic textbook examples are the motion of dislocations in metals, of domain walls in ferroelectrics, the problem of crowdion in a metal, sub-monolayer films of atoms on crystal surfaces, transport in Josephson junctions, the sliding of charge density waves and so on. Sliding friction of solids belongs to this class of systems as well, because the microscopic periodic asperities of the mating surfaces may interlock.

One of the pervasive concepts of modern tribology with a wide area of relevant practical applications as well as fundamental theoretical issues is the idea of free sliding connected with *incommensurability*. When two crystalline workpieces with lattices that are incommensurate (or commensurate but not perfectly aligned) are brought into contact, the minimal force required to achieve sliding (i.e., the *static friction*, F_s) should vanish, provided the two substrates are stiff enough. In this configuration, the lattice mismatch causes the total energy to be completely independent of the relative position of the sliders, whereas hardness can prevent pinning and the associated stick–slip motion of the interface atoms, with a consequent negligibly small frictional force. The remarkable conclusion of frictionless sliding can be drawn, in particular, in the well-explored 1D context of the Frenkel–Kontorova (FK) model (see [1] and references therein). Experimental observation of this kind of *superlubric* regime has recently been reported [2].

Based on the success of this kind of simplified tribological approach [3], the hope is to be able to learn

*Corresponding author.
E-mail address: vanossi.andrea@unimore.it (A. Vanossi).

0301-679X/$ - see front matter © 2007 Elsevier Ltd. All rights reserved.
doi:10.1016/j.triboint.2007.11.008

more from the direct study of microscopic dynamics in similarly simplified 1D models. The substrates defining the sliding interface are modelled as purely rigid surfaces or as 1D (or 2D) arrays of particles interacting through simple (e.g., harmonic) potentials. Despite its extreme idealization, this kind of approach seems able to anticipate features of the actual experimental results or of more complex molecular dynamics simulations of frictional phenomena. In this context, the application of *driven* FK like models (see [4] and references therein), describing the dissipative dynamics of a chain of interacting particles that slide over a rigid periodic substrate potential due to application of an external driving force, has found an increasing interest as a possible interpretative key to understand the atomic processes occurring at the interface of two materials in relative motion. The essential feature of the static and dynamic properties of the FK model consists in the competition between the interparticle interaction (having natural lattice constant b) and the substrate periodic potential (of spatial period a). Indeed, if the former favors a uniform separation b between particles, the latter tends to pin the atom positions to the bottom of the wells, evenly spaced by the period a. This length-scale competition, often referred to as frustration, results in a fascinating complexity of spatially modulated structures. For this *two* competing length-scale system, following the pioneering work of Aubry [5], the tribological properties depend mainly on the value of the winding number a/b being rational (commensurate interface) or irrational (incommensurate interface). Rational interfaces are always ingrained and frictional, whereas irrational interfaces exhibit an "Aubry transition" from frictional to frictionless as the chain stiffness increases.

In real situations, however, such a case of "dry", unlubricated friction is often exceptional. The physical contact between two solids is generally mediated by so-called "third bodies", which may act like a lubricant film. If the third body is a solid lubricant, and in particular a crystalline one, the sliding interface corresponds in fact to a system with *three* inherent lengths: the periods of the bottom and top substrates, and the period of the lubricant layer. As sketched in Fig. 1, in order to study the role of incommensurability among the three interface inherent lengths on the sliding dynamics, we may consider a 1D generalized FK model consisting of *two* rigid sinusoidal substrates, of spatial periodicity a (bottom) and c (top), harassing a chain of harmonically interacting particles, of equilibrium length b, mimicking the confined lubricant. Guided by a similarity with the recent study of the driven quasiperiodic FK model [6], we show that, for sufficiently stiff chain (hard crystalline lubricant), the best low-friction regime is achieved for incommensurabilities a/b and c/a related through non-quadratic irrational numbers (as, for example, the cubic spiral mean [7]) rather than through quadratic irrationals (e.g., the golden mean). This result demonstrates how, in a *three*-length sliding system, the *kind* of interface incommensurability (and not just the distinction between commensurate and incommensurate geometry) can dramatically influence, both quantitatively and qualitatively, the tribological behavior.

2. Model and kinetic friction

In numerical simulations of frictional processes, different approaches may be used to induce motion: a constant-velocity algorithm, where the top substrate is directly forced to slide with a given velocity, or a constant-force algorithm, where the external driving force is applied to the top substrate (or even directly to the lubricant layer), or finally a spring-force algorithm, where the slider is driven through an attached spring moving at constant speed. The latter pulling procedure can be viewed as a way to mimic not only the experimental driving device, but to some degree also the elasticity of the slider.

In this paper, we consider a 1D system of two rigid sinusoidal substrates and a chain of interacting particles embedded between them [8], as shown in Fig. 1. The top substrate of mass M is driven through a spring, K_{ext}, which is pulled with constant velocity V_{ext}. The equations of motion becomes

$$m\ddot{x}_i + \gamma\dot{x}_i + \gamma(\dot{x}_i - \dot{X}_{\mathrm{top}}) + \frac{\mathrm{d}}{\mathrm{d}x_i}\sum_{i\neq j} V(|x_i - x_j|) + \frac{1}{2}\left[\sin\frac{2\pi x_i}{a} + \sin\frac{2\pi(x_i - X_{\mathrm{top}})}{c}\right] = 0, \quad (1)$$

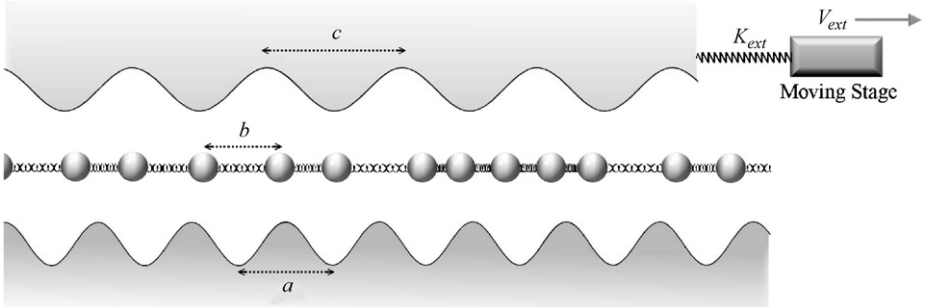

Fig. 1. Schematic drawing of the lubricant chain confined between the two rigid substrates. As shown, the sliding interface is characterized by the three inherent length scales: a, b and c.

$$M\ddot{X}_{\rm top} + \sum_{i=1}^{N}\gamma(\dot{X}_{\rm top} - \dot{x}_i) + K_{\rm ext}(X_{\rm top} - V_{\rm ext}t) + \sum_{i=1}^{N}\frac{1}{2}\left[\sin\frac{2\pi(X_{\rm top} - x_i)}{c}\right] = 0, \quad (2)$$

where x_i $(i = 1, \ldots, N)$ and $X_{\rm top}$ stand for the coordinates of the N chain particles and the top substrate, respectively. The damping γ-terms describe the dissipative forces which are proportional to the relative velocities of the lubricant atoms with respect to both rigid substrates. The viscous coefficient γ represents degrees of freedom inherent in the real physical system (such as substrate phonons, electronic excitations, etc.) which are not explicitly included in the model. The last (sinusoidal) terms represent the on-site interaction between the particles and the substrates. The amplitudes of these rigid potentials are chosen such that the same factor $(\frac{1}{2})$ sits in front of their derivatives in the equations of motion—hence the periodic forces they produce have the same magnitude. The interparticle chain interaction V [fourth term in Eq. (1)] is harmonic with strength K and equilibrium spacing b. We use dimensionless units with chain atom mass $m = 1$ and a bottom substrate period $a = 1$. We focus here on the tribologically most interesting case of the *underdamped* regime, where the damping coefficient γ is much smaller than both characteristic vibrational frequencies of one particle sitting at the minima of the two substrate potentials.

The system is initialized with the lubricant particles placed at rest at uniform separation b. After relaxing the starting configuration, the stage attached to the top substrate through the spring $K_{\rm ext}$, begins to move at constant speed $V_{\rm ext}$. The equations of motion (1), (2) are integrated using the standard fourth-order Runge–Kutta algorithm. After reaching the steady state, the relevant physical characteristics of the system are measured. The detailed behavior of the driven system in Eqs. (1), (2) depends crucially on the length-scale relative ratios a/b and c/a of the substrates and the chain. Since commensurability can only be achieved under well-controlled experimental operating conditions [9], in this investigation we focus on a few specific but typical cases of incommensurability among the three-length scales a, b, c. Specifically we assume a single ratio $a/b = c/a$ and consider the two irrational cases previously studied in the context of the driven quasiperiodic FK model [6], namely the golden mean and the spiral mean [7]. Nevertheless, it should be noted that the qualitative features of the observed dynamics (in a similar 1D confined model corresponding to the $M \to \infty$ limit of Eq. (2), so that in Eq. (1) $\dot{X}_{\rm top} \equiv V_{\rm ext}$) have been shown recently to survive for much more general values of a/b and c/a [10–12], so that this specific choice of incommensurability should not be considered too restrictive. By imposing periodic boundary conditions in order to simulate an infinite system, we are forced to approximate the desired irrational winding numbers a/b, c/a by ratios of integers. Continued-fraction expansion [13] provides a standard and well-established technique to serve this purpose. Quantitatively, a given rational approximant can be checked to be of sufficiently high order to model the desired incommensurability. The chain of N atoms and length $L = Nb$ is thus confined in between the bottom and top substrates with $N_a = L/a$ and $N_c = L/c$ minima, respectively.

In tribology applications, one of the main issues is the kinetic friction force $F_{\rm kin}$ which describes the energy losses inside the contact layer when the substrates move relatively to each other. In our model, $F_{\rm kin}$ can be easily evaluated from energy balance. When the top substrate moves for a distance $\Delta X_{\rm top} = \dot{X}_{\rm top}\Delta t$ relative to the fixed bottom substrate, due to the friction force the system dissipates an energy

$$E_{\rm loss} = F_{\rm kin}\Delta X_{\rm top} = F_{\rm kin}\dot{X}_{\rm top}\Delta t. \quad (3)$$

In the regime of steady motion, this must balance the losses due to the dissipation generated by the γ-damping terms in the chain, i.e.,

$$E_{\rm loss} = \sum_{i=1}^{N}\int_{t_1}^{t_2} {\rm d}t\gamma[\dot{x}_i^2 + (\dot{x}_i - \dot{X}_{\rm top})^2], \quad (4)$$

where $\Delta t = t_2 - t_1$. Thus, for the kinetic friction force, we obtain

$$F_{\rm kin} = \sum_{i=1}^{N}\lim_{\Delta t\to\infty}\int_{t_1}^{t_2}\frac{{\rm d}t}{\Delta t}\gamma[\dot{x}_i^2 + (\dot{x}_i - \dot{X}_{\rm top})^2]\frac{1}{\dot{X}_{\rm top}}. \quad (5)$$

In order to highlight in the kinetic friction force the dissipative part resulting from the internal dynamics of the confined chain, we subtract the systematic contribution arising from the motion of the top substrate, and also normalize $F_{\rm kin}$ to the number of particles N, i.e.,

$$f_{\rm kin} = \frac{F_{\rm kin}}{N} - \frac{1}{2}\gamma\dot{X}_{\rm top}. \quad (6)$$

3. Results

In the range of model parameters considered, our numerical simulations reveal a strikingly different sliding behavior of the system depending on incommensurability. In particular, it is not sufficient simply to distinguish between commensurate and incommensurate periodicities. The "degree" of incommensurability (as measured by continued-fraction expansion) plays a fundamental role as well. Here the mathematical properties of the length-scale ratio leave the realm of abstract number theory to become physically relevant. In the context of the $M \to \infty$ confined model, the peculiar incommensurability-dependent phenomenology has been recently explained [10] by the top slider (meaning here that one among the two substrates whose period c is the longest, so that $b<a<c$) rigidly "dragging" the topological solitons, with linear density $\rho_s = 1/b - 1/a$, that the chain forms with the bottom substrate.

In particular, the choice of incommensurability among the three-length scales a, b, c governs the sliding behavior by inducing a *commensurate* or *incommensurate* matching of the soliton lattice in the chain with respect to the top substrate. In the golden-mean case, $\rho_s c = \phi^2 - \phi = 1$, the soliton lattice is commensurate with the top slider, and so it must ingrain with it. In the spiral-mean case, $\rho_s c = \sigma^2 - \sigma$ is irrational, the soliton lattice is incommensurate with the top slider, and so it can slide freely over it. That describes precisely what happens [14].

Fig. 2 shows the kinetic friction force f_{kin} as a function of the interparticle interaction strength K for different values of the velocity of the moving stage. The plots are given for two irrational choices of the three-length scales: the quadratic golden mean ($N_a = 144, N = 233, N_c = 89$) and the cubic spiral mean ($N_a = 265$, $N = 351$, $N_c = 200$). By simulating larger systems, we checked that these rational approximants [7] are of sufficiently high order to mimic the selected incommensurabilities. In all simulations we set $M = N_c m$, and take $\gamma = 0.2$.

For the *golden* incommensurability, the qualitative (monotonic) behavior of the kinetic friction does not depend significantly on either K or V_{ext}. For the same value of the chain stiffness, f_{kin} decreases with decreasing driving velocity. The chain dynamics exhibits an asymmetric sliding with respect to the two sinusoidal substrates, moving as expected with an intermediate mean velocity, but always faster with respect to the top substrate with the longer spatial period. We checked that the asymmetry persists even when the amplitudes of the substrate potentials are varied significantly with respect to each other. This robust sliding state characterized by a regular time-periodic dynamics, as demonstrated in Fig. 3(b), is specific to the golden incommensurability and to all other quadratic irrationals that we considered. Each single particle in the chain performs exactly the same periodic motion, differing simply by a phase shift. The period $T \approx 26.180$ of the motion is highlighted by the corresponding frequency peak $\nu = (1 - b/a)\, V_{\mathrm{ext}} \simeq 0.038197$ in the Fourier transform of the velocity $\dot{x}_i$ of one generic particle (Fig. 3(c)).

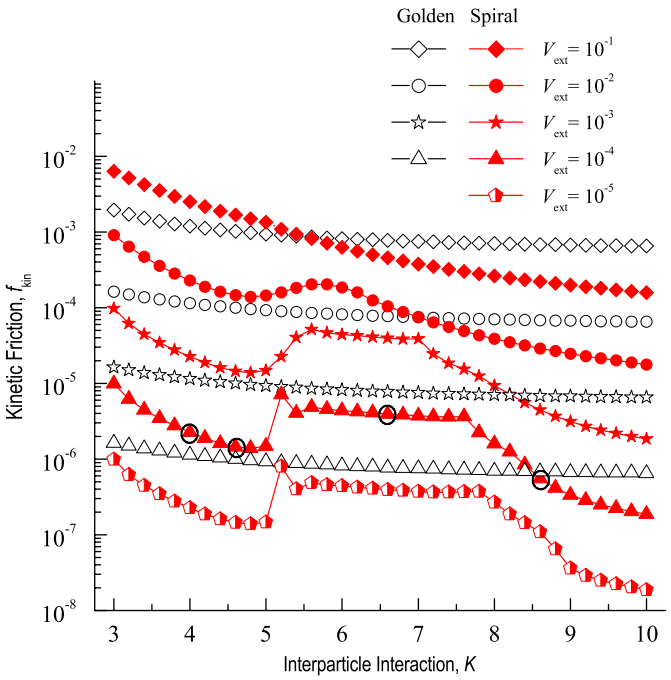

Fig. 2. Dependence of the kinetic friction force f_{kin} on the chain stiffness K for different values of the external driving velocity. Both cases of golden and spiral incommensurability are shown. The black marked circles identify four sliding states whose dynamics has been afterwards analyzed in details.

As anticipated above, specific quadratic irrationals λ, such as the golden mean, occur to satisfy $\rho_s c = \lambda^2 - \lambda = m/n$, so that the soliton lattice and the top slider are commensurate. This commensurability provides an intrinsic ingraining which extends to in principle arbitrarily large chain stiffness, without any transition. As an additional rationale, one may imagine that this particularly strong asymmetric center-of-mass motion is precisely such as to excite, via its time-periodic feature, parametric resonances inside the chain [15], thus converting part of the center-of-mass translational kinetic energy into internal vibrational excitations, making in turn the golden irrationality less favorable to sliding than the spiral one at the values of K considered here.

For inherent lengths related instead by the cubic *spiral* mean, the function $f_{\mathrm{kin}}(K)$ is found to display a non-monotonic and richer behavior, with several different regimes. Only at high driving velocities, $V_{\mathrm{ext}} > 0.01$, these exotic features diminish and eventually disappear. The single-particle motion (see Fig. 3(a)) of the chain, as confirmed by the Fourier spectrum of $\dot{x}_i$ (not shown), is now definitely not periodic. This suppresses the parametric resonances inside the confined layer as possible channels for energy dissipation, making, for stiff chains (large K), the spiral-ratio slider more effective than the golden-ratio one. As noted above, in the spiral case the soliton lattice is incommensurate with the upper slider, and when stiff enough it may actually slide essentially freely over it. The evolution at large K seems in fact towards an almost frictionless smooth sliding. For smaller stiffness, a sharp change in the sliding behavior of the spiral chain is observed at a critical stiffness $K_c \simeq 5.2$, near the value where the Aubry (static depinning) transition for the quasiperiodic FK model was found previously [6]. When the driving velocity decreases (see lower curves in Fig. 2), a plateau region of *larger* dynamic friction $f_{\mathrm{kin}}(K)$ develops, in sharp contrast to the unpinning observed in the static behavior. As can be seen, the location of its left edge is almost independent of V_{ext} and centered around the value K_c. For $K < K_c$ finally the dynamics is characterized by a stick–slip motion. This is consistent with the forced sliding of an incommensurate, but slack and therefore pinned, soliton irregular arrangement. At large and increasing chain stiffness, the spiral friction drops considerably (with a center-of-mass velocity becoming symmetric, i.e., $V_{\mathrm{ext}}/2$), as compared to the golden-mean case: in the latter, friction

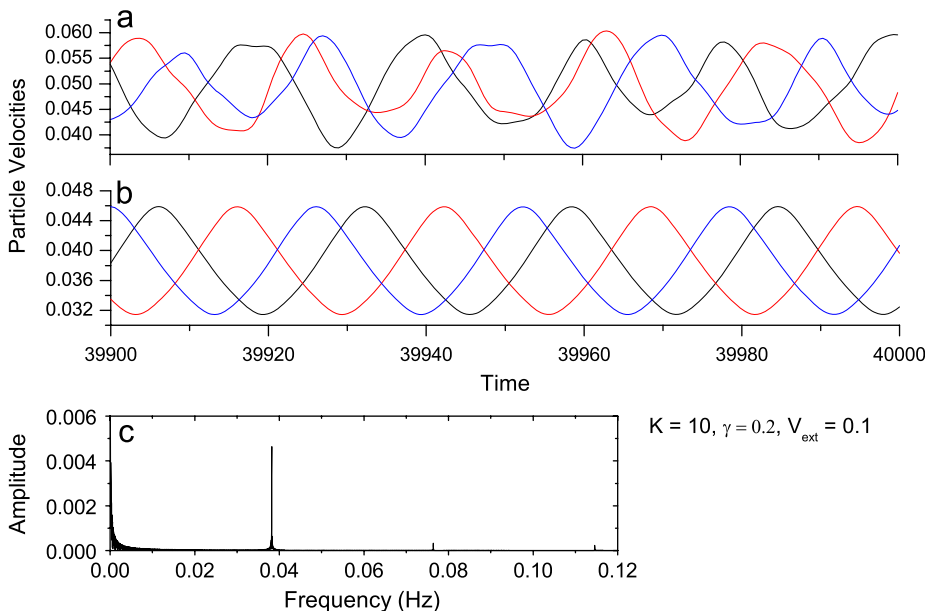

Fig. 3. Atomic velocities versus time for (a) spiral incommensurability $a/b = 351/265$, $c/a = 265/200$; (b) golden incommensurability $a/b = 233/144$, $c/a = 144/89$. For clarity, only the velocities of three adjacent particles of the chain are shown. Panel (c) displays the corresponding Fourier transform of $\dot{x}_i$, showing the sharp peak exactly located at the frequency $\nu = 1/T \approx 0.03819$ that characterizes the time-periodic dynamics of the golden-mean case.

retains quite large values due to the velocity asymmetry of its fully regular time-periodic motion which is not destabilized until strikingly large K.

In order to get more insight into different regions to the left, in between, and to the right of the spiral frictional plateau, we analyze in detail the four points circled in black in Fig. 2, all belonging to the same driving velocity $V_{\text{ext}} = 10^{-4}$. The four upper panels of Fig. 4 show the time evolution of the spring force $F_{\text{ext}} \equiv K_{\text{ext}}(X_{\text{top}} - V_{\text{ext}}t)$; the lower panels display the corresponding velocities of the top substrate and of the center-of-mass of the chain. The first upper panel for $K = 4.0$ clearly displays a typical sawtooth dependence of $F_{\text{ext}}(t)$, the hallmark of stick–slip motion. Stick–slip as a phenomenon is quite general and extremely well known. It has been observed in many simulations of microscopic friction, as well as in the tip dynamics of atomic force microscopy and in surface force apparatus experiments of confined lubricants under shear (see, e.g., Ref. [9] and references therein). Energy is stored in the springs while atoms are trapped in a metastable state (sticking), and it is converted to kinetic energy as the atoms pop to the next metastable state (slipping). The value of the spatial distance covered during the slip events and the regular-periodic or intermittent-chaotic temporal alternation between stick and slip can be affected by several factors: the intrinsic periodicity of the lattices defining the substrate potentials, the potential energy landscape of accessible metastable states, the specific features of imposing driving, etc. At $K = 4.6$ the slip events are prevailing, but the stick–slip regime of the chain is still clearly visible. The next value examined, $K = 6.6$, lies in the plateau region. Here the chain stiffness is too high to support stick–slip, and the confined layer motion reaches a sliding regime with almost constant value of the pulling spring force, and the velocity of the top substrate exhibiting only very tiny oscillations around V_{ext}. The increase in the average kinetic friction f_{kin} of the plateau states (relative to the contiguous stick–slip dynamics region) can be ascribed to the asymmetric chain motion with respect to the two substrates in this regime. In this range of stiffness and driving velocity values, a better dynamical phase-matching is possible between the confined layer and the two sinusoidal substrates, promoting the excitation of dissipative parametric resonances, similar to the golden case. Inside this plateau, even if the detailed particle dynamics still remains irregular (quasiperiodic), a remarkable phase cancellation between the Fourier spectra of different chain particles (all having the same amplitude spectrum, with different phases) yields strictly periodic center-of-mass motion of the embedded chain. Finally, at $K = 8.6$ the confined layer slides almost freely with a very low value of f_{kin}. Sliding becomes symmetric in this regime, i.e., the average chain velocity nearly equals one half of the relative velocity of the two rigid substrates.

4. Conclusions

When two periodic substrates are forced to slide relative to each other but a solid "lubricant" layer is interposed in between, the frictional dynamics of the intermediate layer may display an unexpected behavior, significantly dependent on the incommensurability chosen. Our results show that, depending on physical parameters such as the lubricant stiffness, at least for a three-lengths contact interface (a typical physical situation) there is no quantitative and qualitative uniformity of behavior in incommensurate sliding friction, and that certain incommensurate (e.g., non-quadratic) geometries can favor sliding systematically

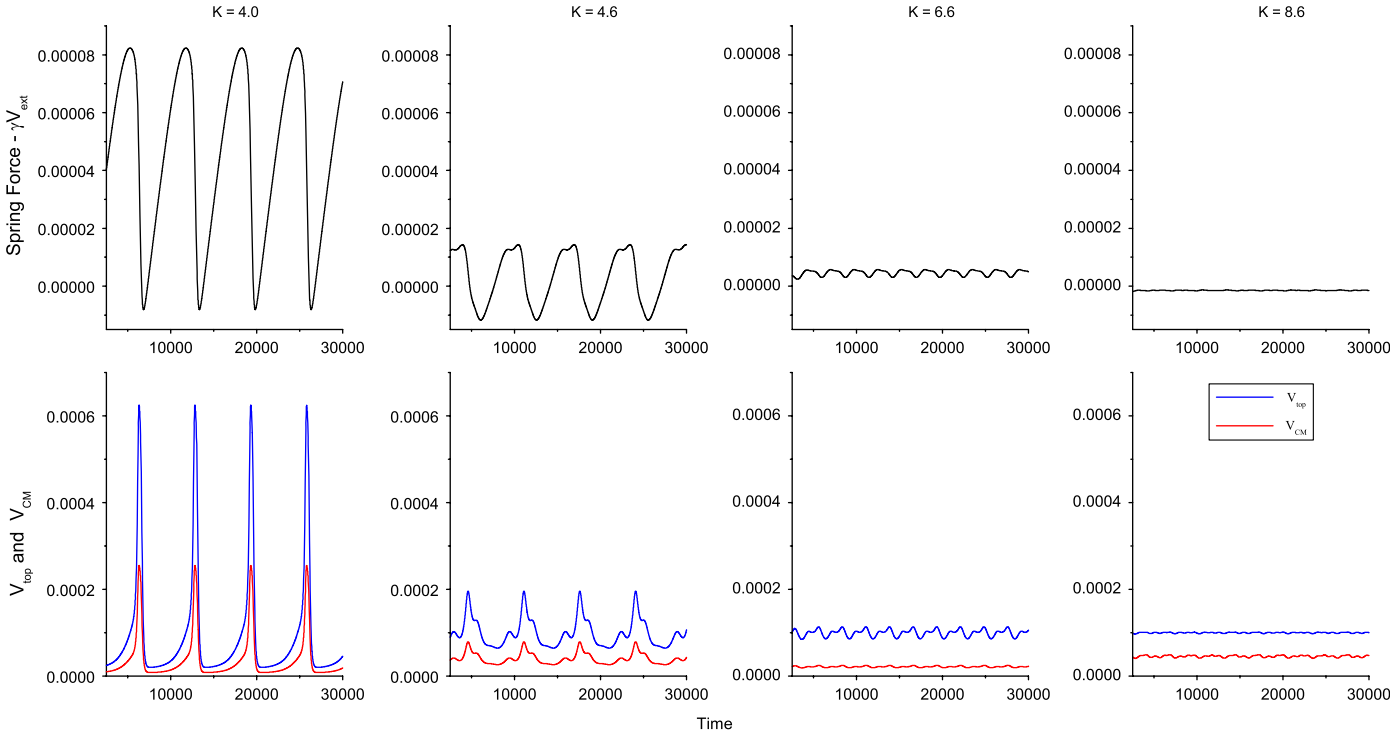

Fig. 4. Dynamics of the four sliding states marked by the black circles in Fig. 2. The four upper panels show the temporal behavior of the spring force, to which the trivial γV_{ext} drift term is subtracted, with the characteristic transition from stick–slip motion at low K (left) to smooth sliding at high K (right). The lower panels display the corresponding time dependencies of the velocities of the top substrate and of the center-of-mass of the lubricant chain.

better than others. In particular, we showed here that for sufficiently stiff confined chains, the standard golden-mean case reveals a higher kinetic friction than the spiral one. This is attributable to the hidden commensurability of the soliton lattice formed between the chain and the lower slider, which occurs in the golden mean but not in the spiral-mean case. From recent preliminary numerical simulations [16], it seems that this conclusion can be generalized from the present 1D case to more significant and realistic 2D interfaces. Similarly to what was recently done for a real two-length sliding contact (graphite flake on graphite) [2], our three-length situation could, in principle, be accessed experimentally by driving, e.g., a graphite flake between two different but well-defined crystalline surfaces.

Acknowledgments

This research was partially supported by PRRIITT (Regione Emilia Romagna), Net-Lab "Surfaces & Coatings for Advanced Mechanics and Nanomechanics" (SUP&RMAN).

References

[1] Braun OM, Kivshar YS. Phys Rep 1998;306:1.
[2] Dienwiebel M, et al. Phys Rev Lett 2004;92:126101.
[3] See, e.g., Vanossi A, Braun OM. Simulation of nanofriction through driven simplified models. In: Buzio R, Valbusa U, editors, Advances in contact mechanics: Implications for Materials Science, Engineering and Biology; 2006 Kerala, India: Research Signpost; (and references therein).
[4] Braun OM, Kivshar YS. The Frenkel–Kontorova model: concepts, methods, and applications. Berlin: Springer; 2004.
[5] Aubry S. Physica D 1983;7:240;
Aubry S, Le Daeron PY. Physica D 1983;8:381.
[6] Vanossi A, Röder J, Bishop AR, Bortolani V. Phys Rev E 2001;63:017203.
[7] The spiral mean ($\sigma \approx 1.3247$) belongs to the class of cubic irrationals, satisfying the equation $\omega^3 - \omega - 1 = 0$. Its rational approximants can be generated by the recursion relation $G_{n+1} = G_{n-1} + G_{n-2}$ with $G_{-2} = G_0 = 1, G_{-1} = 0$. For the golden mean $\phi = (1 + \sqrt{5})/2$, the needed rational approximants are provided instead by the famous Fibonacci sequence $F_{n+1} = F_n + F_{n-1}$ with $F_0 = F_1 = 1$.
[8] Braun OM, Vanossi A, Tosatti E. Phys Rev Lett 2005;95:026102.
[9] Müser MH, Urbakh M, Robbins MO. Adv Chem Phys 2003;126:187.
[10] Vanossi A, Manini N, Divitini G, Santoro GE, Tosatti E. Phys Rev Lett 2006;97:056101.
[11] Santoro GE, Vanossi A, Manini N, Divitini G, Tosatti E. Surf Sci 2006;600:2726.
[12] Manini N, Cesaratto M, Santoro GE, Tosatti E, Vanossi A. J Phys Condens Matter 2007;19:305016.
[13] Khinchin AYa. Continued fractions. New York: Dover; 1997.
[14] Vanossi A, Manini N, Caruso F, Santoro GE, Tosatti E. Phys Rev Lett 2007;99:206101.
[15] Strunz T, Elmer F-J. Phys Rev E 1998;58:1601.
[16] Castelli IE, Manini N, Capozza R, Vanossi A, Santoro GE, Tosatti E. To be submitted.